EVS24
Stavanger, Norway, May 13-16, 2009

Modeling and Simulation of Electric drive System for a Hybrid Electric Combat Vehicle

Yu-seok Jeong[1], Sang-Yong Jung[2], Young-Ryul Kim[3], Byung-Moon Han[4]
[1]*Myongji University, Gyeonggi-do 449-728, Korea, jeong@mju.ac.kr*
[2]*Dong-A University, Busan 604-714, Korea, syjung@dau.ac.kr*
[3]*Hanyang University, Gyeonggi-do 437-718, Korea, yrk1234@hanyang.ac.kr*
[4]*Myongji University, Gyeonggi-do 449-728, Korea, erichan@mju.ac.kr*

Abstract

This paper presents modeling and simulation of electric drive system for a hybrid electric combat vehicle which consists of a diesel engine, a flywheel-type PM generator and its converter, a Li-ion battery pack, six inwheel-type PM motors and their inverters. The six motor/inverter sets are replaced to one set for the simplicity of modeling, since all of them have the same structure. This series hybrid electric drive system combines a diesel engine with Li-ion batteries to deliver high instantaneous output power, enabling faster acceleration than the conventional one. It also can support the stealth mode for silent operation using only battery power, which will be one of the significant features for future combat applications. The diesel engine is modeled with throttle control using SimDriveline and other components are modeled using SimPowerSystems in Matlab/Simulink. This work discusses control features of the PM generator and the PM motor and shows overall behavior of the electric drive system.

Keywords: modeling, simulation, hybrid, electric drive, control

1 Introduction

Hybrid electric drive system (HEDS) expands its territory from automotive industry to military applications. In the United States, the emerging future combat system (FCS) program establishes combat hybrid power system (CHPS) that might provide all the energy and power needs of improved future combat vehicles [1]. Many researches on modeling and simulation of HEDS treat sizing and power management of the drive system [2][3]. Once the components are designed to meet the energy and power requirements, it is followed by the controller design. Among several hybrid configurations, a series type as depicted in Fig. 1 was adopted in this work. A permanent magnet (PM) generator cranks up the engine at standstill and it operates as an alternator after the engine starts. A battery pack links the dc bus between converter output and inverter inputs. A PM motor drives each wheel of the vehicle through a gearbox.

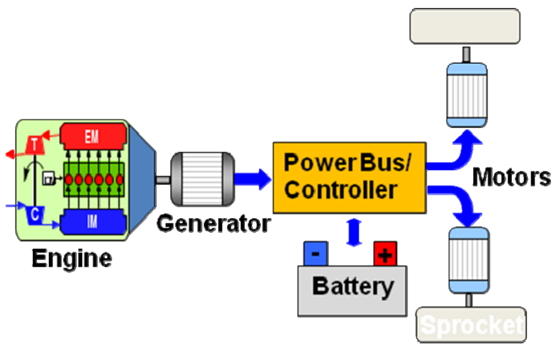

Figure1: Drive system configuration of SHEV

The power converters for generator/motors are controlled to track their torque command. This work discusses modelling and simulation of HEDS and show its dynamic behavior.

2 Modeling of the Electric Drive System

2.1 Diesel Engine model

The diesel engine model uses a programmed relationship between torque and speed modulated by the throttle signal. Even though an actual diesel engine does not have a throttle, its signal specifies the actual engine torque delivered as a fraction of the maximum torque possible in a steady state at a fixed engine speed and indicates the torque demand relative to maximum available torque. If the engine speed rises above the maximum allowed, the output torque is cut to zero. Saturation is applied to keep the throttle signal between zero to one. The actual engine drive shaft speed is fed back to the engine input. The torque-speed curve of the engine is used to determine the maximum torque at the operating speed. Engine torque ripple is modeled with sinusoidal function. The air-fuel combustion dynamics is disregarded for the simplicity of analysis.

2.2 Battery model

The battery model is parameterized to represent a rechargeable battery. It is modelled using a simple controlled voltage source in series with a constant resistance. Even though an actual battery does not have the same characteristics for the charge and the discharge cycle, that of the battery model in this work is assumed to be same. The open voltage source is calculated with a non-linear equation based on the actual state-of-charge (SOC) of the battery [4]. The controlled voltage source is described by

$$E = E_0 - K\frac{Q}{Q-\int i\,dt} + Ae^{-B\int i\,dt} \qquad (1)$$

Where E_0 denotes battery constant voltage, K is the polarization voltage, Q is the battery capacity, A is the exponential zone amplitude, B is the exponential zone time constant, and i is the battery current. The model can accurately represent the battery behaviour, provided the parameters are well determined. The main feature of this battery model is that the parameters can easily be deduced from a manufacturer's discharge curve.

2.3 Generator/Motor model

Three-phase PM synchronous machines are employed in this work and the rotor reference frame is introduced to achieve vector control. The stator voltage model of a PM synchronous machine adopted in the drivetrain can be expressed in the rotor reference frame.

$$\mathbf{v}^{\mathbf{r}}_{\mathbf{dq}} = R_s\mathbf{i}^{\mathbf{r}}_{\mathbf{dq}} + \frac{d}{dt}\boldsymbol{\lambda}^{\mathbf{r}}_{\mathbf{dq}} + \omega_r\mathbf{J}\boldsymbol{\lambda}^{\mathbf{r}}_{\mathbf{dq}} \qquad (2)$$

$$\begin{bmatrix} v_d^r \\ v_q^r \end{bmatrix} = R_s\begin{bmatrix} i_d^r \\ i_q^r \end{bmatrix} + \frac{d}{dt}\begin{bmatrix} \lambda_d^r \\ \lambda_q^r \end{bmatrix} + \omega_r\begin{bmatrix} 0 & -1 \\ 1 & 0 \end{bmatrix}\begin{bmatrix} \lambda_d^r \\ \lambda_q^r \end{bmatrix}$$

where $\mathbf{v}^{\mathbf{r}}_{\mathbf{dq}}$, $\mathbf{i}^{\mathbf{r}}_{\mathbf{dq}}$, and $\boldsymbol{\lambda}^{\mathbf{r}}_{\mathbf{dq}}$ denote the voltage, the current and the flux linkage vector, respectively. The flux linkage can be explicitly expressed as a function of the stator current and the rotor PM flux linkage.

$$\boldsymbol{\lambda}^{\mathbf{r}}_{\mathbf{dq}} = \mathbf{L_s}\mathbf{i}^{\mathbf{r}}_{\mathbf{dq}} + \boldsymbol{\Lambda}_{\mathbf{m}}$$

$$\begin{bmatrix} \lambda_d^r \\ \lambda_q^r \end{bmatrix} = \begin{bmatrix} L_d & 0 \\ 0 & L_q \end{bmatrix} + \begin{bmatrix} \Lambda_m \\ 0 \end{bmatrix} \qquad (3)$$

where L_d, L_q, and Λ_m denote the d- and q-axis inductances and the PM flux linkage, respectively. Having high saliency, PM synchronous machines are magnetically saturated at heavy load. The more the machine is saturated, the lower the inductance is. The flux linkage can be estimated in steady state by

$$\boldsymbol{\Lambda}^{\mathbf{r}}_{\mathbf{dq}} = (\Omega_r\mathbf{J})^{-1}\left(\mathbf{V}^{\mathbf{r}}_{\mathbf{dq}} - R_s\mathbf{I}^{\mathbf{r}}_{\mathbf{dq}}\right)$$

$$\begin{bmatrix} \Lambda_d^r \\ \Lambda_q^r \end{bmatrix} = \frac{1}{\Omega_r}\begin{bmatrix} 0 & 1 \\ -1 & 0 \end{bmatrix}\left(\begin{bmatrix} V_d^r \\ V_q^r \end{bmatrix} - R_s\begin{bmatrix} I_d^r \\ I_q^r \end{bmatrix}\right) \qquad (4)$$

where the capitals denote steady-state variables. Neglecting iron losses for minimum-copper-loss operation, the flux linkage is symmetric to the q-axis current, and the off-line test can be done to estimate the flux linkage in the rotor reference frame.

The electromagnetic torque of a PM synchronous motor can be expressed as

$$\tau_e = \frac{3P}{2}\mathbf{i}^{\mathbf{r}\,\mathrm{T}}_{\mathbf{dq}}\mathbf{J}\,\boldsymbol{\lambda}^{\mathbf{r}}_{\mathbf{dq}} = \frac{3P}{2}\left(\lambda_d^r i_q^r - \lambda_q^r i_d^r\right) \qquad (5)$$

where P denotes the pole pairs of the machine. Thus the torque can be calculated from d- and q-axis current and flux linkages based on the estimation by (4). However, this may not be useful enough to meet the specification of tracking accuracy in torque control due to neglect iron losses. Practically the machine torque is measured during the test to estimate the flux linkage.

The machine capability without iron loss at nominal battery voltage can be estimated by the torque-speed curve using the flux linkage.
The voltage constraint imposed by the power converter can be can be expressed as

$$\left| R_s \mathbf{I}^{\mathbf{r}}_{\mathbf{dq}} + \Omega_r \mathbf{J} \mathbf{\Lambda}^{\mathbf{r}}_{\mathbf{dq}} \right| \le \frac{V_{dc}}{\sqrt{3}} \quad (6)$$

$$\left(R_s I^r_d - \Omega_r \Lambda^r_q\right)^2 + \left(R_s I^r_q + \Omega_r \Lambda^r_d\right)^2 \le \left(\frac{V_{dc}}{\sqrt{3}}\right)^2$$

where V_{dc} denotes the dc link voltage of the power converter and it should be noted that the actual voltage limit represented as a hexagon in the stationary reference frame is approximated to its inscribed circle for the simplicity of analysis.

2.4 Converter/Inverter model

Three-phase power converter is modeled using average technique in a duty level rather than in a pulse-width-modulation (PWM) level to reduce the simulation time of the whole system. The dc input of a power converter is converted to the ac output by PWM technique and space vector PWM among various methods is typically adopted to implement PWM in three-phase switching converters. It allows not only to simplify the control organization, but also to maximize the exploitation of the converter hardware, inherently realizing a third harmonic injection mechanism. The relationship between dc input quantities and ac output quantities in three-phase power converter can be expressed using the duty ratio of each phase.

$$\begin{bmatrix} v_a \\ v_b \\ v_c \end{bmatrix} = \begin{bmatrix} D_a \\ D_b \\ D_c \end{bmatrix} v_{dc} \qquad i_{dc} = \begin{bmatrix} D_a \\ D_b \\ D_c \end{bmatrix}^{\mathrm{T}} \begin{bmatrix} i_a \\ i_b \\ i_c \end{bmatrix} \quad (7)$$

where D_a, D_b, and D_c denote the duty ration of a-, b-, and c-phase, respectively.

3 Controller design

The engine and the PM generator are controlled to meet the demand power determined from the battery SOC and the motor toque. To supply the power the engine torque and the generator speed is respectively controlled, since the dynamic response of the engine is typically slower than that of the generator. The speed controller of the PM generator is arranged as an external control loop around a torque control loop as the cascaded internal loop which has exactly the same structure with that of the PM motor.

The torque of either the generator or the motor is generally controlled by regulating its current. Based on the test data for the flux linkage in (4) and the electromagnetic torque in (5), d- and q-axis current reference in the rotor reference frame can be generated by inverse mapping since the test gives only the maps from d- and q-axis current to the flux linkage and the electromagnetic torque.
Considering the variation of the dc link voltage, the inputs of two-dimensional look-up tables for current references are torque and flux amplitude. In the viewpoint of operating range in mechanical aspects of a PM synchronous machine, however, the motor speed is inversely proportional to its flux amplitude as can be inferred by (6) neglecting the stator resistance at high speed.

$$\Omega_r \le \frac{V_{dc}}{\sqrt{3\left(\Lambda^{r\,2}_d + \Lambda^{r\,2}_q\right)}} \quad (8)$$

As the current reference is actually fixed under the same torque command below the rated speed, the look-up tables is only needed above at the rated speed. Moreover, if the torque is chosen to be the input of the look-up table, its availability decreases as the machine speed increases, and therefore the power instead of the torque is more appropriate for the input of the look-up table.
The current controller is typically designed in the synchronous reference frame which is identical to the rotor reference frame for PM synchronous machines. The current controller has a feedback term to reduce the error between the reference current and the measured one, and a feedforward term to compensate the cross-coupled rotational voltage between d- and q-axis. The resultant current controller designed in frequency domain can be expressed as

$$\mathbf{v}^{\mathbf{r}*}_{\mathbf{dq}} = \left(\mathbf{K_p} + \frac{\mathbf{K_i}}{s}\right)\left(\mathbf{i}^{\mathbf{r}*}_{\mathbf{dq}} - \mathbf{i}^{\mathbf{r}}_{\mathbf{dq}}\right) + \omega_r \mathbf{J} \boldsymbol{\lambda}^{\mathbf{r}}_{\mathbf{dq}} \quad (9)$$

$$\begin{bmatrix} v^{r*}_d \\ v^{r*}_q \end{bmatrix} = \begin{bmatrix} K_{pd} + \frac{K_{id}}{s} & 0 \\ 0 & K_{pq} + \frac{K_{iq}}{s} \end{bmatrix} \left(\begin{bmatrix} i^{r*}_d \\ i^{r*}_q \end{bmatrix} - \begin{bmatrix} i^r_d \\ i^r_q \end{bmatrix} \right) + \omega_r \begin{bmatrix} 0 & -1 \\ 1 & 0 \end{bmatrix} \begin{bmatrix} \lambda^r_d \\ \lambda^r_q \end{bmatrix}$$

where $\mathbf{K_p}$ and $\mathbf{K_i}$ denote the proportional gain matrix and the integral gain matrix.
Assuming that the output voltage of the current controller in (9) is ideally supplied to the PM synchronous machine by the power converter, the tracking characteristic can be expressed by

$$\mathbf{i}_{\mathbf{dq}}^{\mathbf{r}} = \left\{ \mathbf{L}_{\mathbf{s}} s^2 + \left(R_s \mathbf{I} + \mathbf{K}_{\mathbf{p}} \right) s + \mathbf{K}_{\mathbf{i}} \right\}^{-1} \times \left(\mathbf{K}_{\mathbf{p}} s + \mathbf{K}_{\mathbf{i}} \right) \mathbf{i}_{\mathbf{dq}}^{\mathbf{r}*} \qquad (10)$$

It is desirable for d- and q-axis current controllers to have the tracking feature of the fist-order low-pass-filter (LPF) and can be expressed as

$$\mathbf{i}_{\mathbf{dq}}^{\mathbf{r}} = \frac{\omega_c}{s + \omega_c} \mathbf{i}_{\mathbf{dq}}^{\mathbf{r}*} \qquad (11)$$

where ω_c denotes the cut-off frequency of the LPF. Eq. (10) and (11) yield to

$$\mathbf{K}_{\mathbf{p}} = \omega_c \mathbf{L}_{\mathbf{s}} \quad \mathbf{K}_{\mathbf{i}} = \omega_c R_s \mathbf{I}$$

$$\begin{bmatrix} K_{pd} \\ K_{pq} \end{bmatrix} = \begin{bmatrix} \omega_c L_d \\ \omega_c L_q \end{bmatrix} \quad \begin{bmatrix} K_{id} \\ K_{iq} \end{bmatrix} = \begin{bmatrix} \omega_c R_s \\ \omega_c R_s \end{bmatrix} \qquad (12)$$

4 Simulation

The HEDS has been investigated by computer simulation. The engine was modelled using SimDriveline^{TM} and other components using Sim PowerSystem^{TM} in Simulink. The HEDS model is depicted in Fig. 2 and its parameters are shown in Table 1. The converter controls the speed of the PM generator and the inverter controls the torque of the PM motor.

The test condition is cranking of the engine at 0.1sec and driving rated power of the PM synchronous motor from the battery at 0.2sec. The simulation result for HEDS system is shown in Fig. 3, where (a), (b), and (c) show the dynamic behavior of the PM generator, the PM motor and the battery pack. It shows the PM synchronous machine speed, its electromagnetic torque, and dq current in (a) and (b), and shows the battery SOC, the battery current, and the battery voltage in (c).

Table1: Parameters of HEDS

Component	Parameter	Value (unit)
Engine	Power	250(h.p.)
	Torque	840(Nm)
Generator	Power	180(kW)
	Speed	3000(rpm)
Motor	Torque	600(Nm)
	Speed	6000(rpm)
Battery	Capacity	200(Ah)
	Voltage	576(V)

5 Conclusions

The paper has introduced a modeling technique using Simulink for the simulation of an HEDS, which is appropriate to investigate its dynamic feature. The simulation results have demonstrated that this technique is effective to verify its dynamic performance.

Acknowledgments

This work was financially supported by the advanced human resource development program of MKE (Ministry of Knowledge and Economy) through the Research Center for Intelligent Microgrid in Myongji University.

References

[1] M. M. Freeman, "Hybrid power – an enabling technology for future combat system," in *Conf. Rec. of PMS*, pp.1–4, 2000

[2] R. E. Colyer, "The use of electric and hybrid-electric drives in military combat vehicles," in *Journal of Battlefield Technology*, vol. 6, no. 3, pp. 11–14, 2003

[3] S. Fish and T. B. Savoie, "Simulation-based optimal sizing of hybrid electric vehicle

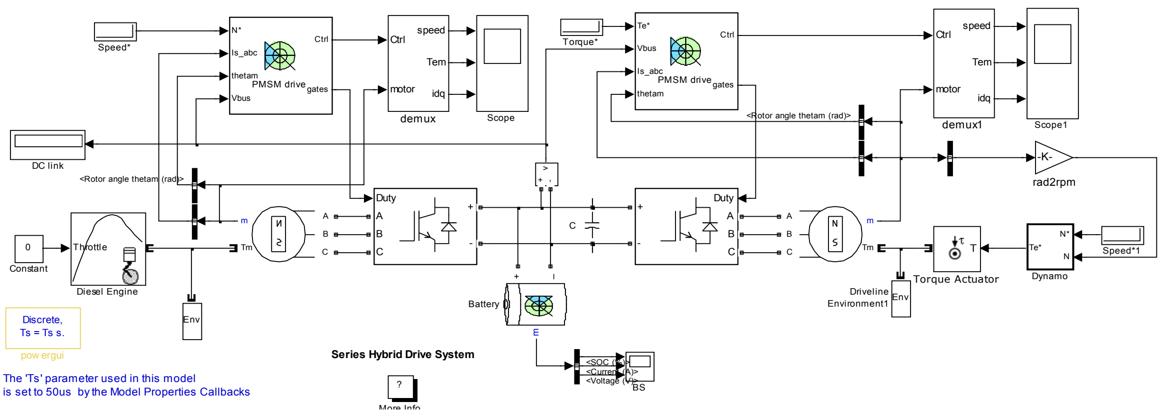

Figure2: Simulation model of HEDS

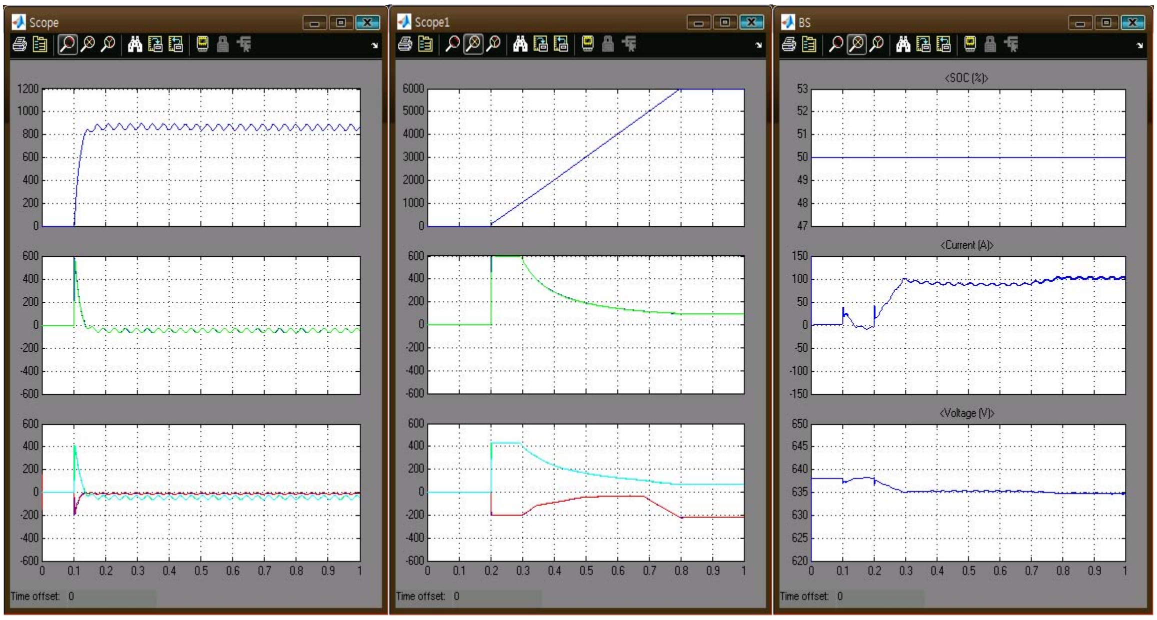

(a) Generator (b) Motor (c) Battery

Figure3: Dynamic behavior of each component for HEDS

Components for specific combat missions,” *IEEE trans. on Magnetics*, vol. 37, no. 1, pp. 485–488, 2001

[4] O. Trembly, L. Dessaint, and A. Dekkiche, “A generic battery model for the dynamic simulation of hybrid electric vehicle,” *IEEE VPPC*, pp. 284–289, 2007

Authors

Yu-seok Jeong received the B.S., M. S., and Ph. D. degrees from Seoul National University, all in electrical engineering. He is currently with the Dept. of Electrical Engr. at Myongji University in Korea. His research interests include modelling and digital control of power electronics and energy conversion.

Sang-Yong Jung received the B.S., M. S., and Ph. D. degrees from Seoul National University, all in electrical engineering. He is currently with the Dept. of Electrical Engr. at Dong-A University in Korea. His research interests include optimal design of PM machines using Finite Element Method.

Young-Ryul Kim received the B.S., M.S. degree in mechanical engineering from Hanyang University, Seoul, Korea and completed Ph.D. degree in system engineering from Ajou University. He has experienced the design and control of power system in the field of vehicle and robot. He is currently with the Cim & Robotics Lab. at Hanyang University.

Byung-Moon Han received the B.S. degree in electrical engineering from Seoul National University, Seoul, Korea, in 1976, and the M.S. and Ph. D. degrees from Arizona State University in 1988 and 1992, respectively. He is a professor in the Dept. of Electrical Engineering, Myongji University in Korea. His research interests include the high-power power electronics and FACTS.